International Journal of Innovation and Applied Studies
ISSN 2028-9324 Vol. 8 No. 3 Sep. 2014, pp. 1094-1111

http://www.ijias.issr-journals.org/

Potential climate change impacts on water resources in the Buyo Lake Basin (Southwest of Ivory Coast)

Tanoh Jean-Jacques Koua[1-2], Jean Patrice Jourda[1], Kan Jean Kouame[1], Kouao Armand Anoh[1-3], Daniela Balin[2], and Stuart N. Lane[2]

[1]Laboratory for Remote Sensing and Spatial Analysis Applied to Hydrogeology, Félix Houphouet-Boigny University of Cocody-Abidjan, Ivory Coast

[2]Faculty of Geosciences and Environment, University of Lausanne, Lausanne, Switzerland

[3]Swiss Federal Institute of Aquatic Science and Technology (Eawag) Dubendorf, Switzerland

ABSTRACT: The sensitivity of subtropical African river basins to possible future climate change is a matter of some concern. In Ivory Coast, previous works on climate change impacts predict a decrease in annual average water resource by the 2080s between 6.9% and 8.4%. This is a potentially serious issue because of a series of historical resource management decisions that have increased dependence upon water use, such as through major dam building schemes. This paper focuses upon the Buyo Lake catchment, a central resource for the Ivorian people with the aim of providing future water resource scenarios, under climate change so as to develop appropriate adaptation policies. The study applied simulations from the UKMO climate model, HadGEM1 from the ENSEMBLES project 2009, with the A1B emissions scenario in continuous simulation. Daily climate data such as rainfall, temperature, wind speed and relative humidity were input to the SWAT hydrological model. The simulations were performed after model calibration. Analysis focuses on the periods 1950-1979 (baseline), 2035-2064 (2050 horizon) and 2064-2093 (2080 horizon).The results showed that the entire basin of Buyo could experience a serious temperature elevation of +1.34°C by the 2050s and +3.87°C by the 2080s. A reduction in the available water resource is therefore projected. Thus precipitation is forecast to fall by c. 10.3 % in the 2050s and 14.9 % in the 2080s as compared to the baseline period. Evapotranspiration is expected to increase by 3.6% and 3.4% respectively for the 2050s and 2080s. Runoff is forecast to decrease about 27.7 % for the 2050s and 40.0% in the 2080s. Recharge to groundwater is also forecast to fall by 34.2 % to the 2050s and 45.8% to the 2080s.This could lead to the drying up of groundwater aquifers. These changes are potentially serious and emphasise the need to develop adaptation strategies to prepare for future climate change.

KEYWORDS: Climate change, Water, Modeling, Simulation, Buyo, Ivory Coast, Watershed.

1 INTRODUCTION

Water is one of the main current and future challenges facing Africa. The water supply from rivers, lakes and rainfall is not equally accessible, the natural geographical distribution is uneven and water consumption cannot be called sustainable. Climate change is likely to impose additional constraints on the availability and accessibility of water in terms of quantity and quality. In West Africa, the first simulations let glimpse a small variation in rainfall compared to the current rainfall. This decrease in rainfall greatly depending on the latitude, varies from 0.5 to 40% of the annual rainfall over the period 1961-1990. A downward trend in rainfall was observed from the late 1960s/early 1970s until the early 1990s [1], [2], [3], [4]. Deficits were estimated at 16% for tropical Africa, 16% in 1980s and 7% in the 1970s. The mean temperature and climate

variability are projected to increase, due to climate change. However, for the changes in mean rainfall, climate models do not yet provide consistent results [5]. There is evidence from meteorological observations and modeling that the total annual rainfall may decrease in the sub-humid regions in West Africa within the next decades. This applies also to the small West-African country Ivory Coast. In the 2080-2099 horizons, flows in West Africa, calculated based on the A1B emission scenario could fall to 50% [5]. According to [6], although forecasts regarding runoff and groundwater recharge vary greatly regionally following the anticipated changes in precipitation and materials according to climate models, most climate change scenarios indicate the decrease in flow and groundwater recharge in arid and semi-arid areas of West Africa. Thus, the river flows will decrease in proportions varying between 5 and 34% depending on the time horizons and countries [6]. The most vulnerable regions are mainly countries bordering the Gulf of Guinea [7]. It is important to note that these predictions have not 100% accurate, but give a coherent plausible future, with the choice of emission scenarios. However, recently studies using IPCC models on West Africa [8] by comparing the annual cycle and the trends observed and simulated precipitation and average monthly temperatures, we conclude that six (6) models best simulate observations of rainfall and temperature: CGCM3.1, GFDL-CM2.0, GISS-EH, GISS-ER and UKMO-HadGEM1. In Ivory Coast, research has highlighted the impacts of climate variability on water and the environment [9], [10], [11], [4], [12], [13], [14].Thus, a gap of 21 % was observed in the rain [4]. The decrease in runoff can reach above 20% [5]. Specifically, the flow regime in the 2075 horizon of Sassandra at Piébly and Kahin (Western Ivory Coast) could decrease by 8.4% and 6.9% [15], [16].These variations have negative effects on the hydrological cycle, and so upon environment and socio-economic activities. One of the major issues raised by research on a complex phenomenon such as climate change is to quantify its impact upon the hydrological cycle and water resources. Thus, in this study, it was discussed to assess the possible future impacts of climate change on water resources in Buyo Lake watershed with the SWAT model, using data from UKMO HadGEM1-A1B climate scenarios from IPCC ENSEMBLES project. UKMO HadGEM1 climate model has never been applied especially to Buyo Lake basin. This study is the first trial to evaluate possible impacts of climate change upon water balance under A1B emission scenario.

2 MATERIALS AND METHODS

2.1 STUDY AREA

The study area is located in the South-western Ivory Coast between latitude 5°57' and 8°26' North and longitudes 6°45'and 7°51' West (Figure 1). The basin is located in the Guinean climate zone and its surface is estimated at about 24,560 km^2. This zone has two equatorial rainfall maxima (June and September) and belongs to the whole Sassandra River watershed. On average, this watershed has between 2,000 to 2,500 mm of precipitation per year [17]. The main geological groups are composed of amphibolite, anorthosite, gneiss, granitoid, itabirite, metasediments, migmatite, metavulcanite and schists. The basin is composed of four (4) main soil types: brown soils, lateritic soils highly desaturated, hydromorphic lateritic soils and lateritic soils moderately desaturated [18]. These types of soils favor the development of agriculture.

2.2 MATERIALS

The first data to use was the Digital Elevation Model (DEM) (Figure 2). The DEM is from the UTM projection, Zone 30, Northern Hemisphere resolution of 93 meters. It is obtained by downloading from the internet web site: http://srtm.csi.cgiar.org/SELECTION/inputCoord.asp. It is used to delineate the basin, to subdivide the basin into subbasins and to extract the hydrographic network. The land use map used in this study is for the year 2000 at the scale 1/200 000 (Figure 3), was provided by the CCT (Centre for Mapping and Remote Sensing), a specialized Ivorian Establishment in the map design. Eight major classes are so identified. The dominant classes are Agricultural land (42.30%), Range-Brush (29%) and Forest-Mixed (17.22%) [19].The soil map (figure 4) was obtained mainly from the Harmonized World Soil Database (HWSD) developed by the Food and Agriculture Organization of the United Nations (FAO-UN) [20]. Twenty three units of soil are then extracted and completed by additional informations from literature and national soil documents. The hydro meteorological data used in this study are the maximum and minimum temperature, precipitation, relative humidity, solar radiation and wind speeds with a daily time step both for the SWAT calibration model and the prospective simulation by using the UKMO-HadGEM1 climate model. The SWAT calibration data were obtained throughout the http://globalweather.tamu.edu/ SWAT web site (Figure 5).These data cover the period 1980-2010.The data for the prospective simulation with 1.875° x 1.25° as resolution, were obtained from the website: http://cera-www.dkrz.de/WDCC and were calculated by using the UKMO-HadGEM1 climate model. The periods are: the baseline period (1950-1979), 30 years, representing the past climate and periods representing future climate over the medium term (2035-2064) and long term (2064-2093). From a strictly global view, the scientific community has identified the period 1961-1990 as baseline period. This choice is based primarily on the fact that climatic conditions during this period are relatively stable. In hydrology, we do not find such a consensus on the choice of a baseline period. In the literature, climate and hydrological conditions of the present time are calculated for a

range of reference periods [21]. As daily data observations of temperature and rainfall were available for 1950-1979, we chose this period as the baseline.

2.3 METHODOLOGY

The method employed is based on the SWAT hydrologic model that uses data from climate model UKMO-HadGEM1 as input. The hydrological model SWAT (Soil and Water Assessment Tool), developed by the "United States Department of Agriculture (USDA), Agricultural Research Service" is a tool for water management in the watershed. It is a semi-distributed, semi-physical and semi-empirical model, which operates at a daily time step [22]. SWAT allows: (1) integrated water management (quantity and quality), (2) management of agricultural practices, (3) simulation of large, heterogeneous watersheds, (4) management of surface water and groundwater and (5) modeling processes related to sediment, nutrients and pesticides. SWAT is used worldwide and is supported by a broad scientific community. It is coupled with a GIS (Geographical Information System) with ArcView GIS 3.2a or Arcgis 9.x of ESRI, which allows:

- Easy access to variables and parameters, as spatio-temporal data can be pretreated; design input files and visualization of spatial outputs;
- A spatial emissions and transfers of pollutants, enabling prioritization of areas according to a sensitivity criterion or a degree of action priority. In addition, its source code is freely available.

SWAT includes a hydrological component based on the water balance equation (1):

$$SW_t = SW_0 + \Sigma (R_{day} - Q_{surq} - E_a - W_{seep} - Q_{gw}) \quad (1)$$

With, SW_t = final quantity of water in the ground (mm), SW_0 = initial amount of water in the soil (in mm), R_{day} = total precipitation (mm), Q_{surq} = total runoff (mm), E_a = Total evapotranspiration (mm), W_{seep} = amount of water within the soil unsaturated area (mm), Q_{gw} = amount of water returning to the ground (mm)

The methodology used in this study can be summarized in (2) major steps: **(1) SWAT hydrological model calibration**; **(2) SWAT hydrological model projection with HadGEM1-A1B climate model:**(a) data preparation for the prospective simulation; (b) correction of bias in the climate model UKMO-HadGEM1; (c) preparation of the SWAT hydrological model projection database; (d) simulation with model calibrated parameters; and (e) analysis of the potential impacts of climate change upon water resources.

2.3.1 SWAT HYDROLOGICAL MODEL CALIBRATION

To run SWAT model, we need daily maximal and minimal temperature, precipitations, relative humidity, wind speed and solar radiation. The calibration was done with the SWAT-CUP (SWAT-Calibration Uncertainty Program). The Calibration parameters is automated by SUFI2 (Sequential Uncertainty Fitting version 2) from [23], an integrated method in SWAT-CUP program. Sixteen (16) parameters were then used in this study taking into account the literature on the use of SWAT model in the tropics [24]. The parameters used concern those related to flow. These parameters are: CN2 (curve number 2) ALPHA_BF, GW_DELAY, GW_QMN, GW_REVAP, ESCO, CH_N2, CH_K2, ALPHA_BNK, SOL_AWC, SOL_K, SOL_BD, SURLAG, SLSUBBSN, EPCO and REVAPMN:

- CN2: the SCS curve number is a function of soil permeability, land use and historical soil water status. SCS defines three antecedent moisture conditions: I-dry (wilting point), II-average moisture, and III-wet (field capacity on the ground). CN2 is the moisture condition II (medium moisture);
- ALPHA_BF: base flow factor in days: constant base flow recession, α_{gw} is a direct index of the response of the groundwater flow in the evolution of recharge [25];
- GW_DELAY: Groundwater delay in days. This time cannot be directly measured. It is estimated by simulation comparing simulated and observed variations in groundwater;
- GW_QMN: Threshold depth of water in the shallow aquifer required for the resurgence of flow (mm);
- GW_REVAP: Evaporation Coefficient of groundwater;
- ESCO: Soil evaporation compensation factor: that coefficient has been incorporated to allow the user to modify the depth distribution; it is used to compensate the evaporation of soil application and take into account the effect of capillarity, scabs and cracks;
- CH_N2: Manning coefficient for the main channel;
- CH_K2: Effective hydraulic conductivity in main alluvium channel;

- ALPHA_BNK: coefficient of depletion in the rivers banks;
- SOL_AWC: available water capacity of the soil layer;
- SOL_K: soil hydraulic conductivity at saturation;
- SOL_BD: soil wet density;
- SURLAG: response time of the watershed
- SLSUBBSN: Average slope length (m);
- EPCO: evapotranspiration compensation factor for plant uptake as a function of depth;
- REVAPMN: Threshold evaporation from groundwater (mm)

SUFI2 is a method whose implementation in the field of hydrological modeling involves several steps (Figure 6):

Step 1: In the first step, an objective function is defined. SUFI2 gives us the possibility of using the objective function of our choice between R^2, Chi2, NS, R^2 multiplied by the line regression coefficient b, bR^2, SSQR (sum of squared errors) coefficients. In this study we chose the NS and R^2 coefficients. NS has allowed us to assess the strength of the model predictions and R^2 indicates the correlation between the model simulations and observed values. Two other factors have also been used, R factor and d factor to analyze uncertainties in the simulations;

Step 2: It is to choose the physically meaningful values of the parameters to be optimized, between a minimum and maximum value. There is no theoretical basis for the exclusion of a particular distribution. However, due to the lack of information, we assume that all parameters are uniformly distributed in a region bounded by the minimum and maximum values, they must be as wide as possible, but physically significant (2):

$$bj: b_{j,\ abs\_min} \leq bj \leq b_{j,\ abs\_max} j = 1....m, \qquad (2)$$

where b_j is the j^{th} parameter and m is the number of parameters to be estimated.

Step 3: Following step 2, the Latin Hypercube sampling method [26] is carried out, leading to the desired combination of n simulations. This number must be relatively large (about 500-1500). The simulation program is then executed n times and the simulated output variables of interest, corresponding to the measurements are recorded.

Step 4: In this step, the objective function, g, is calculated.

Step 5: here, is calculated the overall sensitivity of each parameter in each simulation. First, the sensitivity matrix J, of g (b) is calculated using:

$$Jij = \frac{\Delta gi}{\Delta bj} \qquad i = 1,..., C^n_2, \quad j = 1,..., m \qquad (3)$$

Where C^n_2 is the number of lines of the sensitivity matrix (equal to all possible combinations of two simulations) and j is the number of columns (number of parameters).

Then, the equivalent of a Hessian matrix, H is calculated according to the Gauss-Newton and neglecting higher order derivatives as:

$$H = J^T J \qquad (4)$$

Based on the Cramer-Rao theorem [27], an estimate of the lower bound of the parameters covariance matrix, C, is calculated from:

$$C = S^2_g (J^T J)^{-1} \qquad (5)$$

Where S^2_g is the variance of the values from the objective function resulting from n simulations.

The sensitivities of the parameters were calculated according to the system of multiple regressions, which regresses the parameters generated by the "Latin Hypercube" sampling against the values of the objective function:

$$g = \alpha + \sum_{i=1}^{m} \beta ibi \qquad (6)$$

A statistical test is then used from the relation (6) to identify the relative importance of each parameter bi which is the sensitivity parameter.

Step 6: In this step, measures assessing uncertainties are calculated. The calculations are concerning the d factor and R factors. They are calculated at 2.5% (Xl) and 97.5% (Xu) percentile of the cumulative distribution of each point simulated. The goodness of fit is assessed by the uncertainty measurement calculated from the percentage of measured data framed by the minimum and maximum values of the '95PPU (95 percent prediction uncertainty which represents the d factor)', and the average distance between the top and bottom of 95PPU determined from:

$$dx = \frac{1}{k}\sum_{i=1}^{k}(Xu - Xl) \quad (7)$$, where k is the number of observed data points.

The best result is that 100% of the measurements are covered by 95PPU, and close to zero. However, due to measurement errors and uncertainties in the model, the ideal values are generally not achieved. A reasonable measure of d factor, based on our experience, is calculated by the R factor expressed as:

$$Rfactor = \frac{dx}{\sigma x} \quad (8),$$ where σ_x is the standard deviation of the measured d.

A value less than 1 is a desirable measure for the R factor. The calibration was done on the period from 1985 to 1988, about four years. The overall application of the SUFI2 algorithm can be summarized as in figure 6.

To use the calibrated model to estimate the impact of climate change on the flow, the model was validated by trying to reproduce monthly flows observed over a period which has not been used for calibration. The periods chosen for validation are 1989-1992 for the wet period, and 1994-1999 for dry period. The performance of SWAT was evaluated using statistical and stochastic measures to determine the quality and reliability of predictions compared to observed values. Statistical measures used are R^2 (relation 9) and the Nash-Sutcliffe (NS) coefficients (relation 10). To these coefficients were added stochastic parameters (uncertainty) associated with random events such as rain. These parameters are the d factor and the R factor. A model is said to be perfect if the values of R^2 and NS are 1. However, because of errors due to uncertainties in the measurements, it is impossible to reach this value. Thus, some authors [28], [29] consider that NS and R^2 values above 0.5 are acceptable. The theoretical values of the d factor are between 0 and 100%, while those of the R factor are between 0 and infinity. A d factor of 1 and an R factor of zero indicate that the simulation exactly corresponds to the measured data. The degree to which we are far from these figures can be used to assess the robustness of our calibration. A larger d factor can be achieved against a bigger R factor. Thus, often, a balance must be struck between the two so that the simulation is acceptable [23].

$$R^2 = \frac{(\sum_{i=1}^{n}(Yo-Ym)(Ys-Ysm))^2}{\sum_{i=1}^{n}(Yo-Ym)^2\sum_{i=1}^{n}(Ys-Ysm)^2} \quad (9)$$

Y_o: observed value
Y_m: observed mean value
Y_s: simulated value
Y_{sm}: average simulated value

$$NS = \frac{\sum_{i=1}^{n}(Yo-Ym)^2-\sum_{i=1}^{n}(Ys-Ym)^2}{\sum_{i=1}^{n}(Yo-Ym)^2} \quad (10)$$

2.3.2 SWAT HYDROLOGICAL MODEL PROJECTION WITH HADGEM1-A1B CLIMATE MODEL

Data (minimum and maximum temperature, precipitation, wind speed, daily relative humidity) from the UKMO-HadGEM1 model were available with a 1.875° x 1.25° resolution (figure7). These netcdf formats data were converted to .dbf using the tool "Multidimension Tool" of ArcGIS.

Climate models contain bias (Figure 8). Then, these biases were corrected following [30]:

$$T_{d,m}^{scen} = \overline{T_{d,m}^{obs}} + (\overline{T_m^{GCMscen}} - \overline{T_m^{GCMcon}}) \quad (11)$$

$$P_{d,m}^{scen} = P_{d,m}^{obs}.\left(\frac{\overline{P_m^{GCMscen}}}{\overline{P_m^{GCMcon}}}\right) (12)$$

$T_{d,m}^{obs}$ and $P_{d,m}^{obs}$ are daily observed temperatures and precipitation, $\overline{T_m^{GCMcon}}$ and $\overline{P_m^{GCMcon}}$ are the average monthly temperature and rainfall from climate model in the baseline period, $T_m^{GCMscen}$ and $P_m^{GCMscen}$ are the average monthly temperature and rainfall from climate model in the future, $T_{d,m}^{scen}$ and $P_{d,m}^{scen}$ are respectively the scenario daily temperatures and precipitation after correction.

After bias correction, the next step of the study was the preparation of the database required to run the SWAT prospective model for the periods 1950-1979 (baseline), 2035-2064 (2050 horizon) and 2064-2093 (2080 horizon).The new database prepared, helped to reconfigure the watershed; and the SWAT prospective model was run one time on the three periods above, using the calibrated parameters from SWAT hydrological calibration (table 1) to assess the possible impacts of the climate change upon the water resources. This section concerned the analysis of potential impacts of climate change on the main components of the water balance *i.e.* precipitation, actual evapotranspiration, runoff and infiltration in the watershed. Indeed, once the simulation is completed, annual and interannual average outputs of these components were exported to Excel to build graphs needed to interpret the results. The analysis focused on interannual averages of the main water balance components listed above.

Table 1. Rank and optimal values of calibrated SWAT parameters

Rank	Parameter	Parameter Name	Lower bound	Upper bound	Optimal value given by SWAT
1	CH_N2	Manning's "n" value for the main channel	-0.01	0.3	0.0653
2	SURLAG	Surface runoff flag time	0.05	24	0.476
3	CN2	SCS runoff curve number	35	98	37.47
4	REVAPMN	Threshold evaporation from groundwater (mm)	0	500	0.0519
5	ALPHA_BNK	Baseflow alpha factor for bank storage	0	1	0.062
6	CH_K2	Effective hydraulic conductivity in main channel alluvium.	-0.01	500	19.356
7	GW_REVAP	Groundwater "revap" coefficient	0.02	0.2	0.0675
8	SLSUBBSN	Average slope length	10	150	10.285
9	SOL_K	Saturated hydraulic conductivity	0	2000	0.5139
10	ESCO	Soil evaporation compensation factor	0	1	0.8102
11	EPCO	Moist bulk density	0	1	0.6065
12	GWQMN	Treshold depth of water in the shallow aquifer required for return flow to occur (mm)	0	5000	0.4364
13	SOL_AWC	Available water capacity of the soil layer	0	1	0.3531
14	ALPHA_BF	Baseflow alpha factor (days)	0	1	0.0448
15	SOL_BD	Moist bulk density	0.9	2.5	1.5635
16	GW_Delay	Groundwater delay (days)	0	500	415.20

3 RESULTS

3.1 SWAT HYDROLOGICAL MODEL CALIBRATION

A sensitivity analysis was first applied to the sixteen parameters. The results of the sensitivity analysis showed that the most sensitive for the swat model station N'Zo Kahin parameters are: the manning coefficient for the main channel (CH_N2), the response time of the watershed (SURLAG), the scs curve number (CN2) (figure 9a). at piébli station, the most sensitive parameters are the CH_N2, the SURLAG, CN2 (figure 9b). we note from these two graphs figures that the CH_N2, SURLAG and CN2 parameters are most sensitive to flow at the both stations. Thus, the flow is more dependent on hydraulic characteristics of the catchment area. Against by, the GW_Delay, ALPHA_BF, SOL_AWC and GWQMN parameters that govern groundwater flow are less sensitive and influence very little water flow. Once the most sensitive parameters identified, the calibration was performed. The calibration model was performed with 1500 iterations. Then the calibration parameters were used to calibrate the model. The result of the calibration of monthly flow at N'zo Kahin station over the period (1985-1988) shows a correlation coefficient R^2 of 0.89, a Nash coefficient equal to 0.87 (Figure 10), a R factor equal to 0.37 and a d factor of 0.32 . At Piébli station, the result of calibration in the same period indicated a Nash of 0.80 and a correlation coefficient R^2 of 0.82 with R factor and d factor, respectively equal to 0.46 and 0.34 (figure 11). At the wet validation period (1989-1992) (Figure 12), the results obtained at N'zo Kahin station indicates Nash 0.79, an R^2 coefficient of 0.80, with an R factor of 0.39 and 0.21 as d factor. The validation of the hydrological model at Piébli station in wet period gave Nash coefficient of 0.40 and a correlation coefficient R^2 of 0.46 (Figure 13). The measurement uncertainties were evaluated using the R factor and the d factor respectively equal to 0.31 and 0.50. Then the hydrological model was validated on the dry period (1994-1999) to show the ability of SWAT to simulate the climate variability. The result of the validation of the hydrological model in dry period (1994-1999) (Figure 14) gave at N'Zo Kahin station a Nash of 0.63 and a correlation coefficient R^2 of 0.65. The evaluation of

uncertainties in model predictions gave a d factor of 0.40 and an R factor of 0.64. Statistical and stochastic (uncertainty) evaluation of the model is summarized in Table 2. Statistics have shown that there is generally a good correlation between the observed and simulated monthly flow during the calibration and the validation. At Piébli station, Nash and R^2 coefficients are greater than 0.50 in calibration; but during validation, they are slightly lower than 0.50. However, overall, the results could be acceptable and used for planning and protection of water resources of the basin. Indeed, we can say that the SWAT model has been successfully applied in the basin of Buyo Lake in terms of flow calibration.

Table 2. Summary of evaluation criteria

Stations			**N'ZoKahin**				**Piébli**			
	N'Zo Kahin	**Piebli**	**NS**	**R^2**	**d Factor**	**R Factor**	**NS**	**R^2**	**d Factor**	**R Factor**
Calibration	1985-1988	1985-1988	0.89	0.87	0.32	0.37	0.80	0.82	0.34	0.46
Validation (wet period)	1989-1992	1989-1991	0.79	0.80	0.21	0.39	0.40	0.46	0.31	0.50
Validation (dry period)	1994-1999	-	0.63	0.65	0.40	0.64	-	-	-	-

3.2 SWAT HYDROLOGICAL MODEL PROJECTION WITH HADGEM1-A1B CLIMATE MODEL

The temperature changes in the Buyo basin was also treated and gives an overview of the monthly cycle variations of temperature over the 2035-2064 and 2064-2093 horizons (Figures 15 and 16). Indeed, the 2035-2064 horizon, the differences between the average monthly temperatures and those of 1950-1979 are between 25 and 27.2°C, a change from 0 to 1.34°C. The estimated monthly temperature is up to 27.2 °C. The most significant variations are observed in January (1.19°C), March (1.21°C) and December with 1.34°C.

In the 2064-2093 horizon, temperatures estimated by the SWAT model are between 27 and 28.5°C.The variations could be between 0.83 and 3.87°C. The largest variation is in the month of September, which is also the hottest month with an average monthly temperature of 28.5°C.The estimation of the water balance was made for the entire watershed of Buyo Lake. The main parameters namely precipitation (P), actual evapotranspiration (ETR), runoff (R) and infiltration (I) were taken into account. The results of the evolution of the interannual average parameters in the basin for the baseline (1950-1979), 2050 and 2080 horizons are presented in Figure 17.The figure shows that overall, rain, runoff and infiltration decrease for the 2050s and 2080s. In terms of rain, there is a progressive decrease from 1449 mm for the reference period to 1300 mm for the 2050s and 1233 mm for the 2080s, 10.3% and 14.9% respectively. For both of the 2050s and the 2080s, there is an increase in evapotranspiration, rising by 3.6% to the 2050s and 3.4% to the 2080s. The latter is surprising, but it suggests that by the 2080s, the forcing of evapotranspiration rates by temperature rise becomes limited by the availability of precipitation and suggesting a fundamental shift in the hydrology of the basin by the end of the period. The net result is a progressive rise in the percentage of rainfall lost by the basin through evapotranspiration from 59.3% in the baseline period to 68.5% on the 2050s and 72.1% in the 2080s. Given this increase loss by evapotranspiration, it is not surprising the Figure 17 shows systematic reductions in both runoff and groundwater recharge (Figure 17), which decreases from an average of 339.8 mm in the reference period to 245.6 mm in the 2050s and to 204.0 mm in the 2080s. Similarly, groundwater recharge decreases markedly from 249.9 mm in the baseline period to 164.5 mm in the 2050s and 135.4 mm in the 2080s. The focus on mean changes in Figure 17 overlooks interannual variability which may be more important in terms of climate change adaptation. Figure 18 shows the frequency distribution for the baseline, 2050s and 2080s. The graph shows an important distinction between the 2050s and 2080s. By the 2080s, there is a systematic shift in the frequency distribution: that is all years have less rainfall. But, for the 2050s, it is mainly the drier years that become drier, with the wetter years experiencing less change and the most extreme, wettest years, not changing at all. The frequency distribution for evapotranspiration shows that the major changes in evapotranspiration occur between the baseline period and the 2080s but that also the increases in evapotranspiration tend to be greater at frequencies where the evapotranspiration is lower. This confirms that the years with the most extreme evapotranspiration do not see increases in evapotranspiration because these are already limited by available precipitation. The frequency distribution for runoff clearly reflects the changes in precipitation. It shows that between the baseline period and the 2050s, there is an increase in the inter-annual variability of runoff: that is, there is an increase in the number of years with very low runoff. But, it is still possible to have years with relatively high runoff. By the 2080s, runoff in all years has decreased such that the inter-annual variability has returned to levels typical of the baseline period. It should be emphasized that this change is important in terms of water resources. It is possible that for the 2050s, adaptation to those years when there is runoff reduction compared to normal is possible because there remains the possibility that there will be more normal wetter years that follow. However, by the 2080s, all years experienced substantial runoff reduction with approaching 60% of years in the 2080s having less runoff than the year with the smallest runoff in the

baseline period. Groundwater recharge has similar results to those for runoff: there is an initial increase in inter-annual recharge variability to the 2050s, associated with more years when there is less recharge. This then falls to the 2080s as all years show a decrease in recharge. Given that groundwater stocks are slowly replenished, groundwater systems can commonly average out interannual variability, which means that the changes to the 2050s may be less serious than the 2080s when a systematic decrease in groundwater recharge is forecast for all years.

4 DISCUSSION

The analysis of the temperature under the A1B scenario gave variations between 0 and +1.34°C for the period 2035-2064 and +0.83 to +3.87°C in the period 2064-2093. The monthly average temperatures could be affected rising to reach 29°C. This result shows that the watershed could be warm. The temperature variations obtained under 2050s horizon remain well below those of the 2080s horizon. The results of this study confirm those from [7] on the Comoé watershed (Ivory Coast) using the A1B scenario. Thus, according to this author, the 2091-2100 horizon, the expected changes in temperature would be more marked. Indeed, the average monthly differences between the horizon 2091-2100 and the period 1991-2000 will be higher than the 2031-2040 horizon and will be all above 2.8°C. Maximum variations (4.8°C) could be reached. The average annual variation in this horizon is 3.6°C. In addition, the temperature increases calculated in this study are consistent with those provided by [5] and [31] through climate models that global temperature could increase up 1.4 to 5.8°C by 2100s. Most alarmist projections even announce that these increases could reach up to 6.4°C by 2100 [5].The analysis of potential impacts of climate change on the water balance for the 2050s and 2080s was conducted using the emission scenario A1B climate model UKMO-HadGEM1. The results of this study showed that the entire watershed of Buyo Lake could experience a serious change in available water resources. The clearest driver behind this is the forecast precipitation decrease in a basin that due to its geographical location has a very high evapotranspiration rate. Whilst the evapotranspiration rate is forecast to increase, it becomes limited by the declining precipitation in the 2080s scenario. These results are consistent with those from previous work. Indeed, in the domain of major rivers flows, a decrease is observed. By the 2080s, flows in West Africa, calculated based on the A1B emission scenario could fall to 50% of baseline levels [5]. The most vulnerable regions are mainly countries bordering the Gulf of Guinea [7].The modeled decrease is consistent with the results from [32] in the Senegal for the Gambia and Sassandra watersheds, and [16] in the Bandaman (Ivory Coast) watershed and [7] for the Comoé watershed (Ivory Coast).

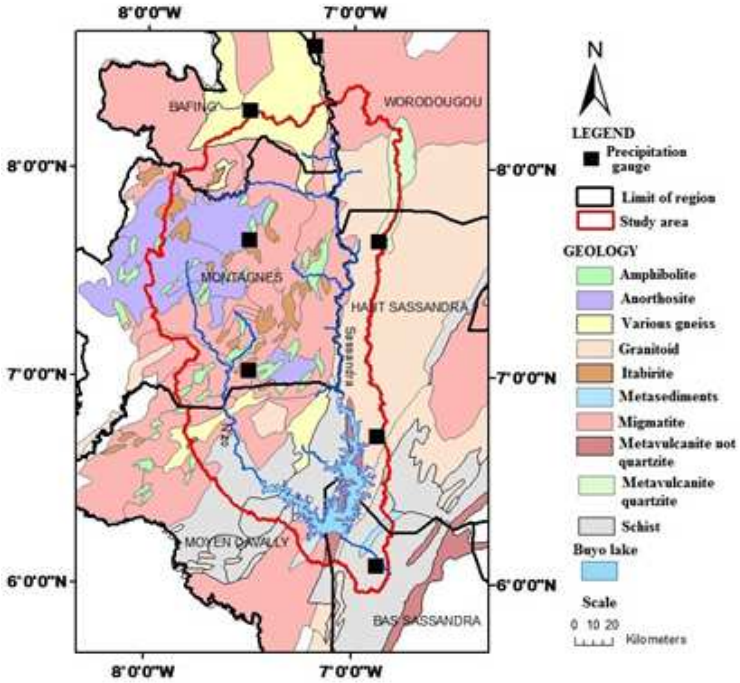

Fig. 1 Buyo Lake Basin

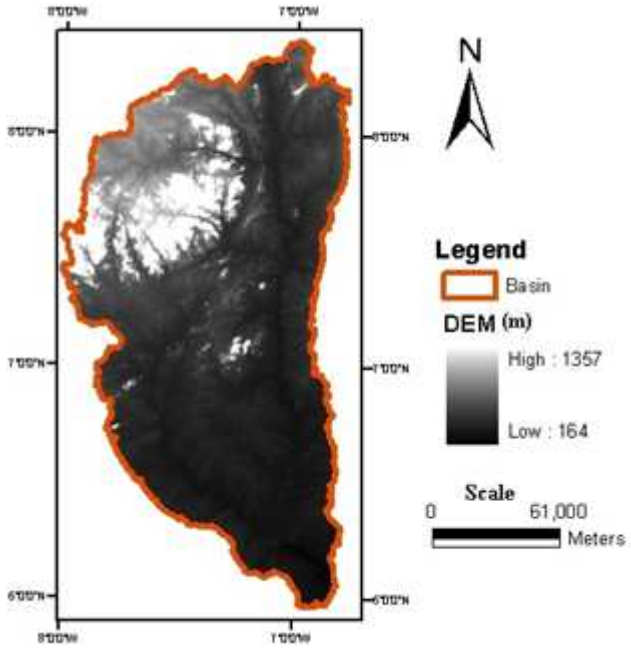

Fig. 2 Digital Elevation Model (DEM) of the watershed

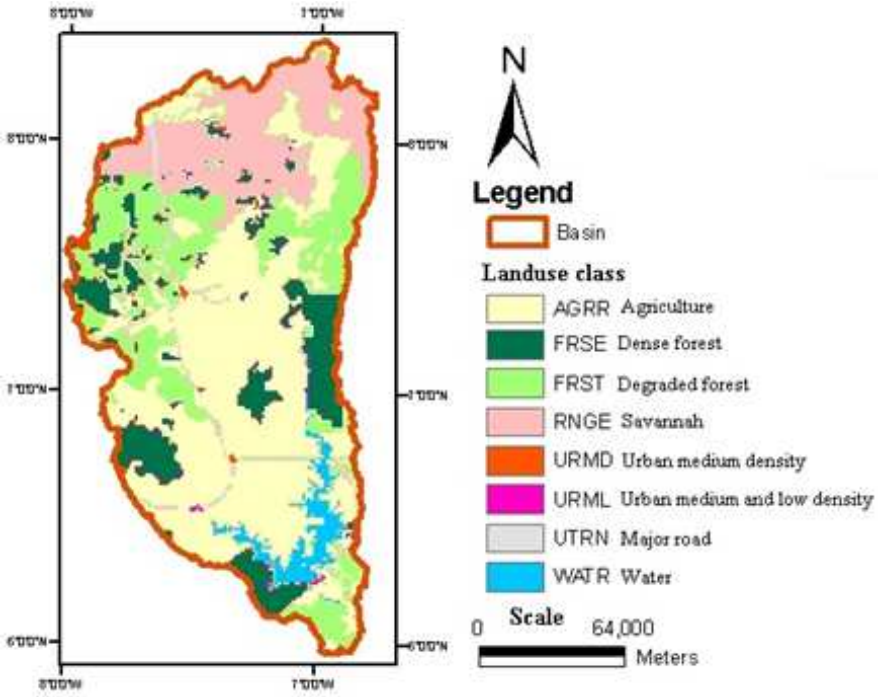

Fig. 3 Land use map of the Buyo Lake watershed

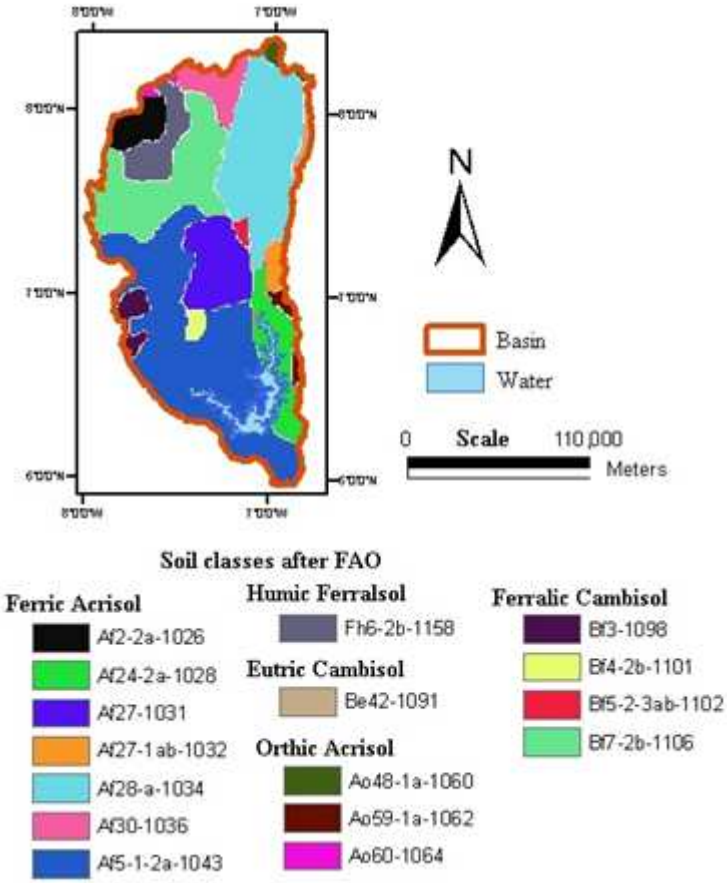

Fig. 4 Soil map of the study area

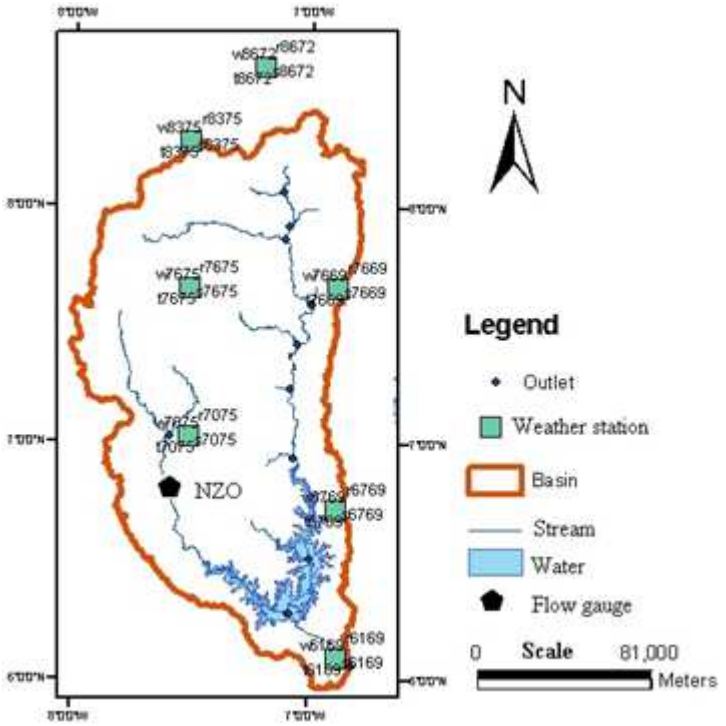

Fig. 5 Location of weather station and flow gauge

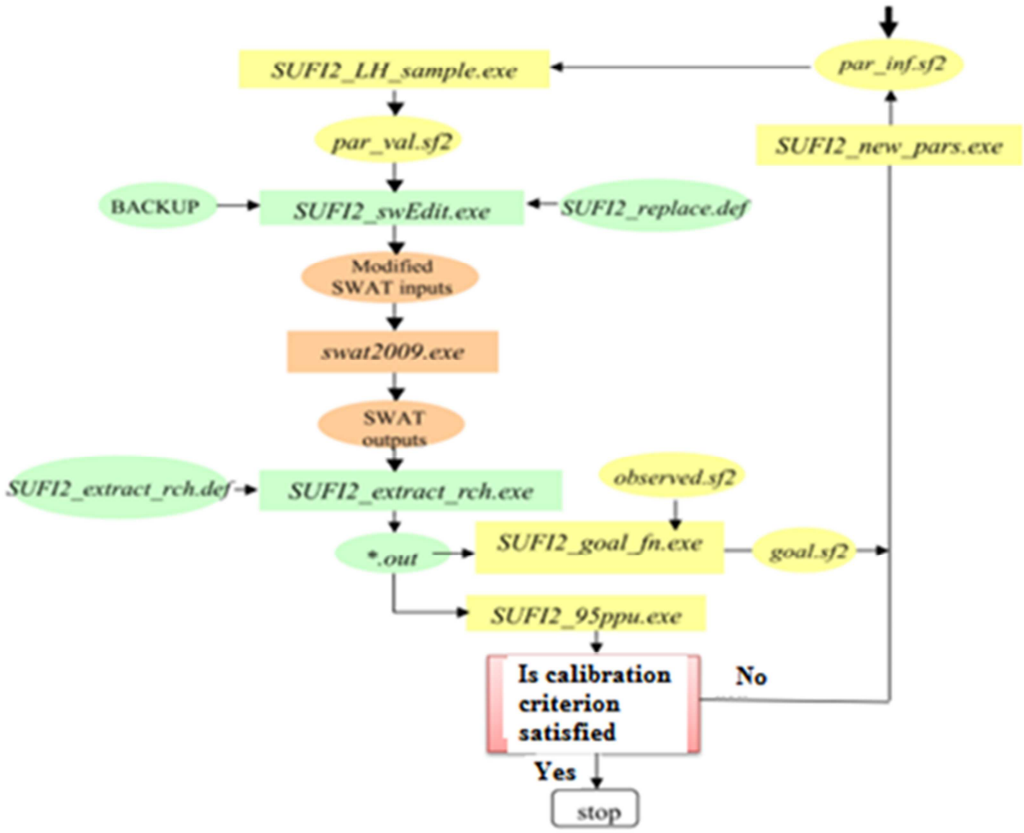

Fig. 6 calibration procedures using the method in the interface SUFI2 SWAT-CUP (Modified Abbaspour, 2011)

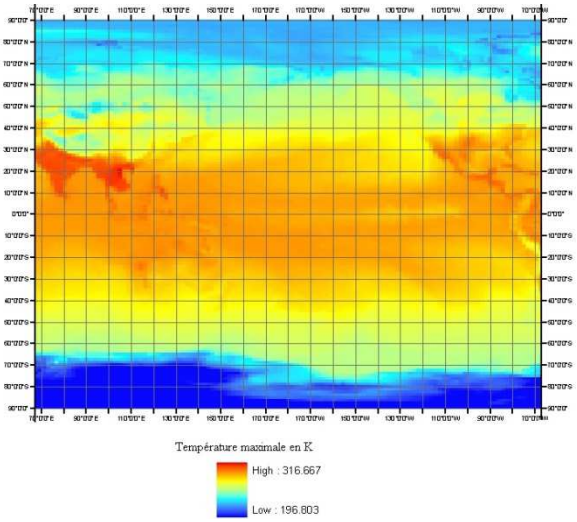

a- Minimal temperature

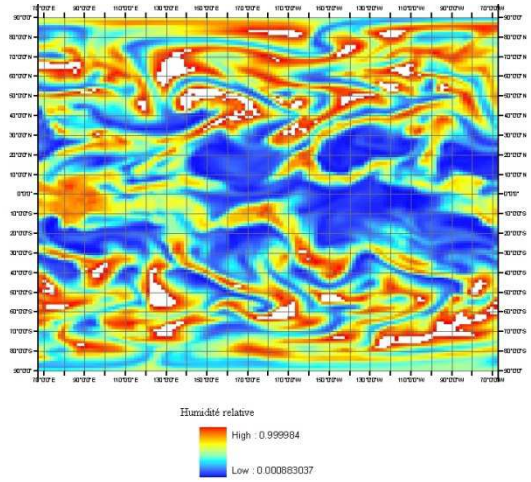

b- Relative humidity

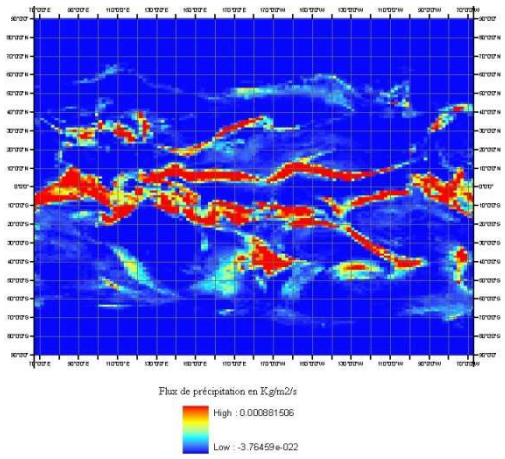

c- Precipitations

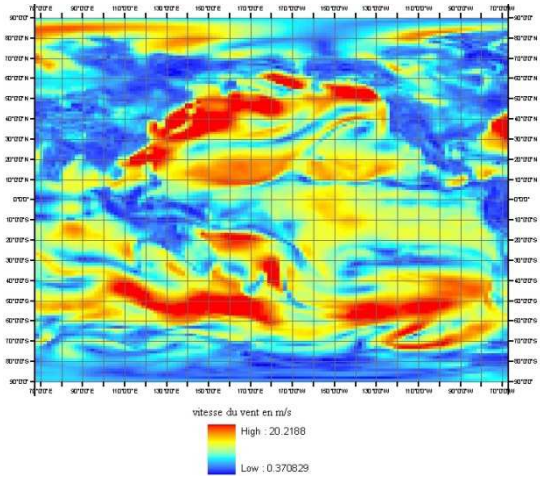

d- Wind speed

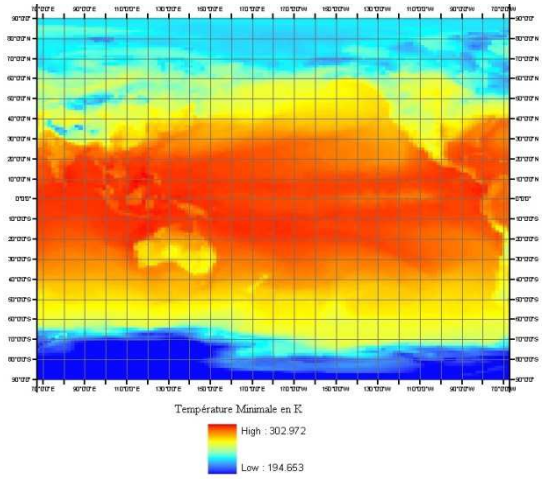

e- Maximal temperature

Fig. 7 Climate Data to NetCDF from climate model UKMO-HadGEM1

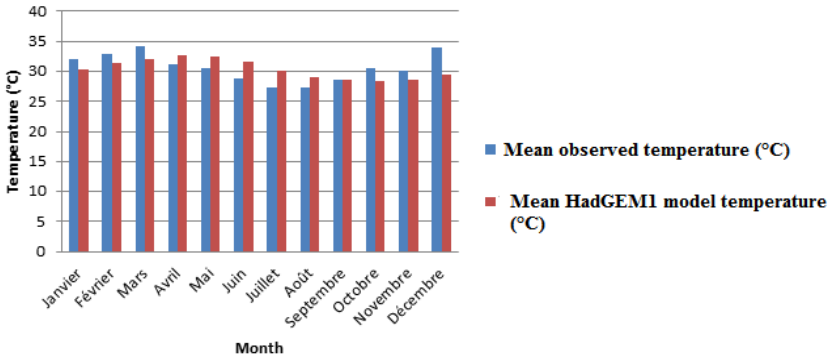

a- Comparison between temperature values from the model and those HadGEM1 observation Watershed Lake Buyo

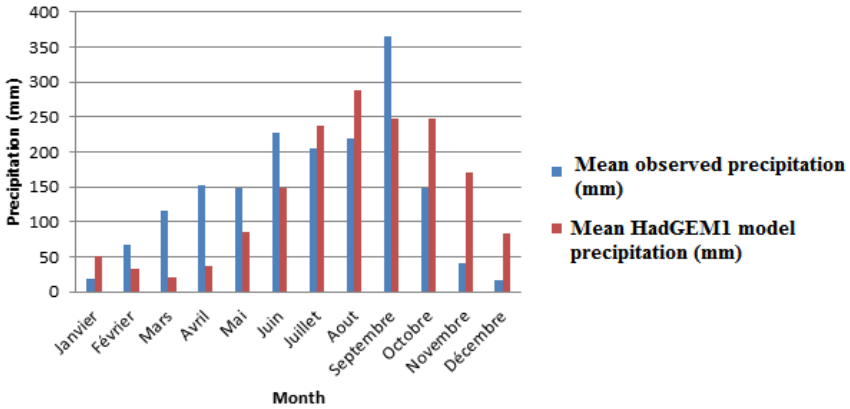

b- Comparison between rainfall values from the model and those HadGEM1 observation Watershed Lake Buyo

Fig. 8 Highlighting HadGEM1climate model bias in the watershed of Lake Buyo

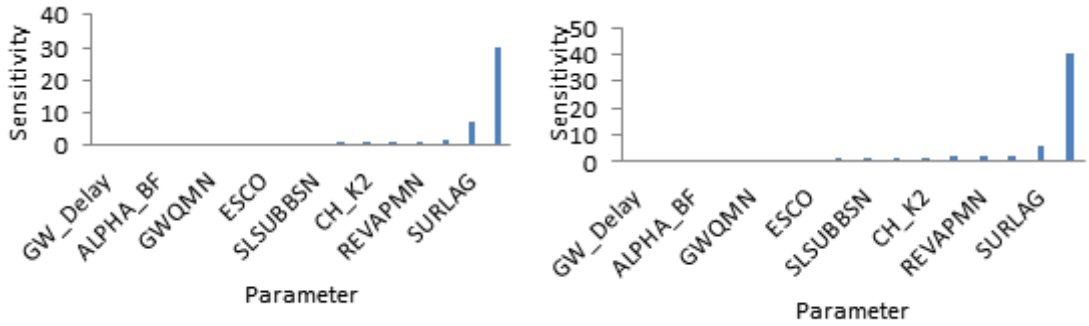

a. Sensitivity parameters to the station N'zo Kahin *b. Sensitivity parameters to the station Piébli*

Figure 9 Sensitivity of flow parameters

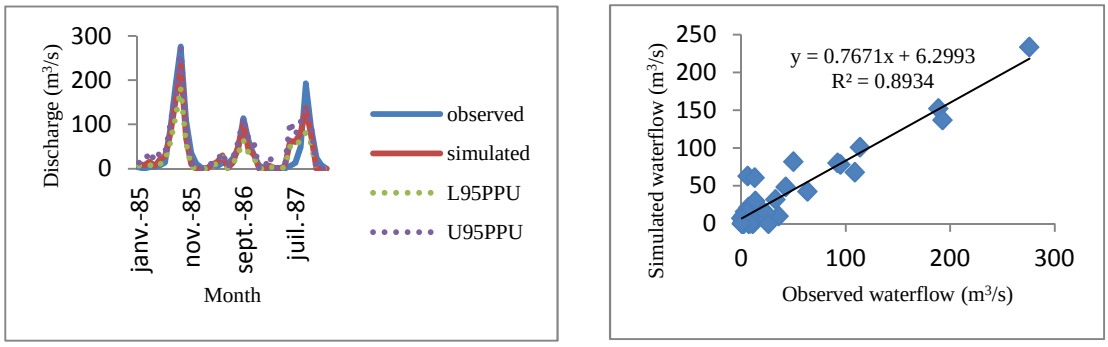

Fig. 10 Calibration of the monthly flow at the gauging station N'Zo Kahin

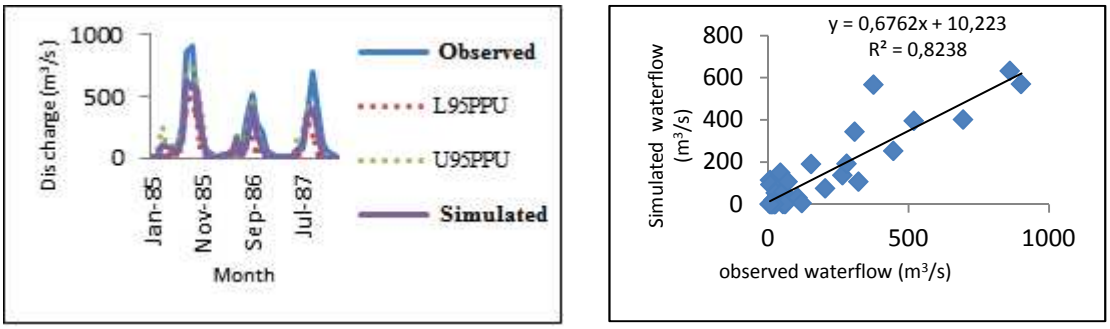

Fig. 11 Calibration of the monthly flow at the gauging station Piébli

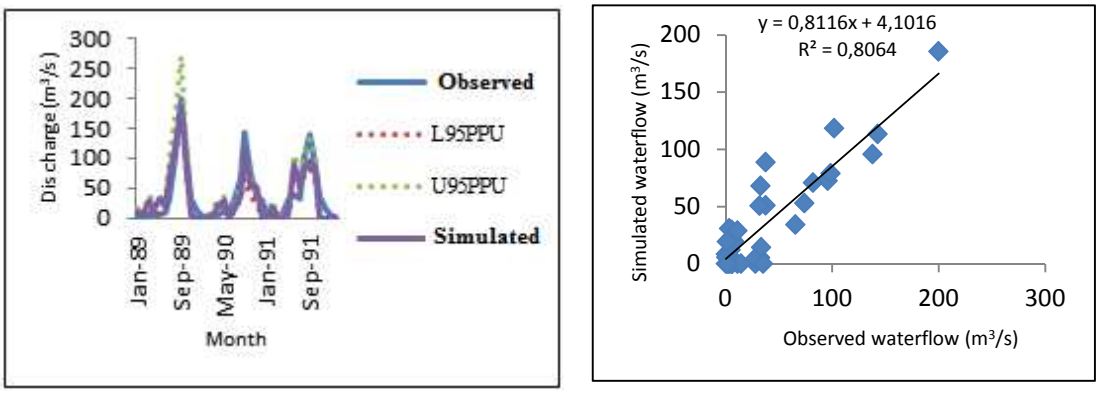

Fig. 12 Validation of the monthly flow at the gauging station N'Zo Kahin wet period (1989-1992)

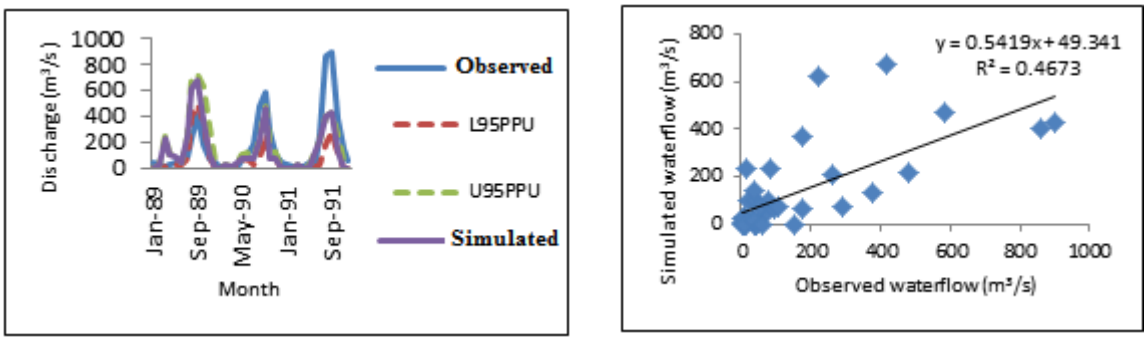

Fig. 13 Validation of the monthly flow gauging station Piébli wet period (1989-1992)

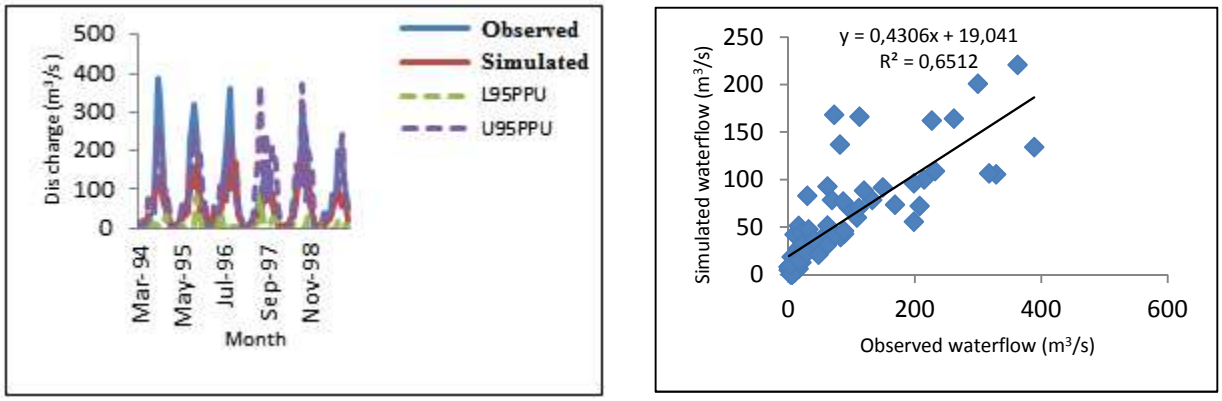

Fig. 14 Validation of the monthly flow gauging station N'Zo dry period (1994-1999

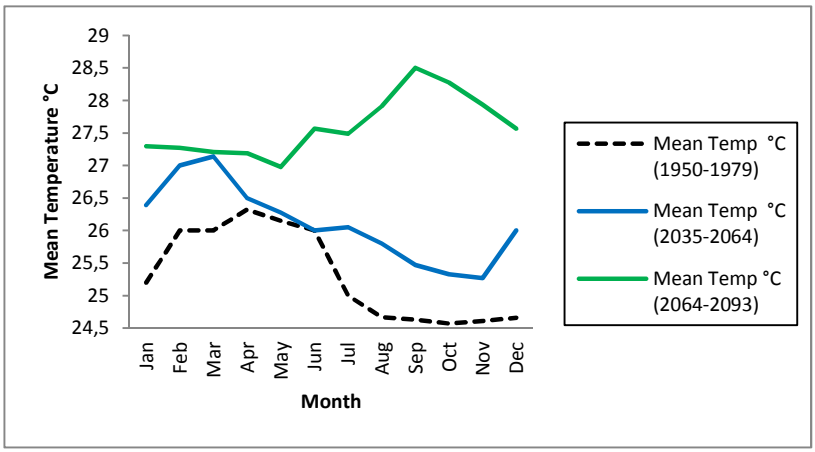

Fig. 15 Evolutions average monthly temperatures in the watershed of Lake Buyo over the period from 2035 to 2064 and from 2064 to 2093

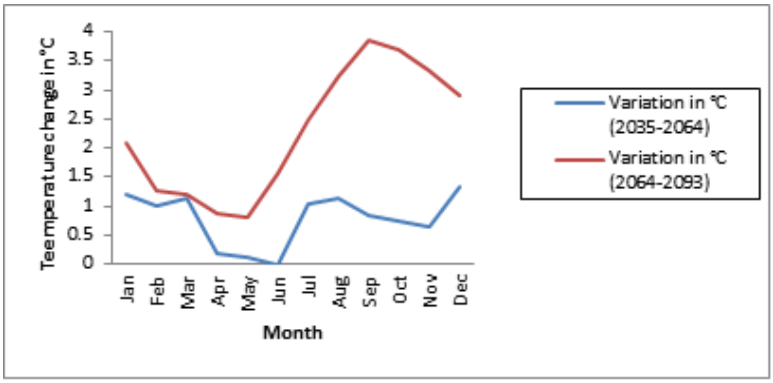

Fig. 16 Changes in average monthly temperatures on the periods 2035-2064 and 2064-2093

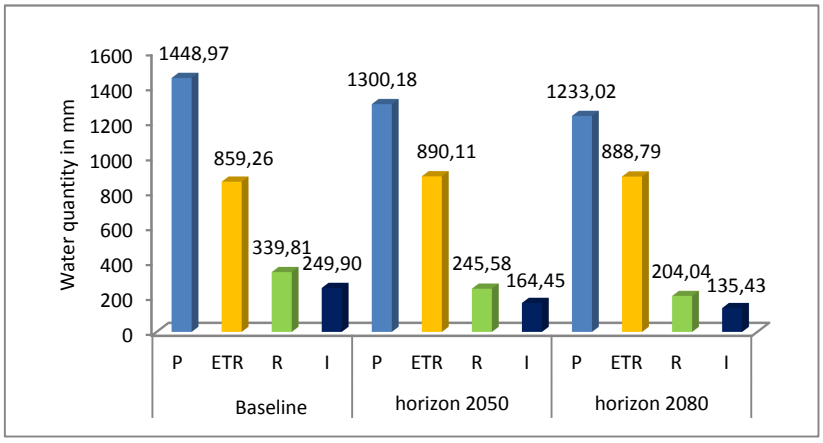

Fig. 17 Changes in the parameters of the water balance in the Buyo Lake watershed

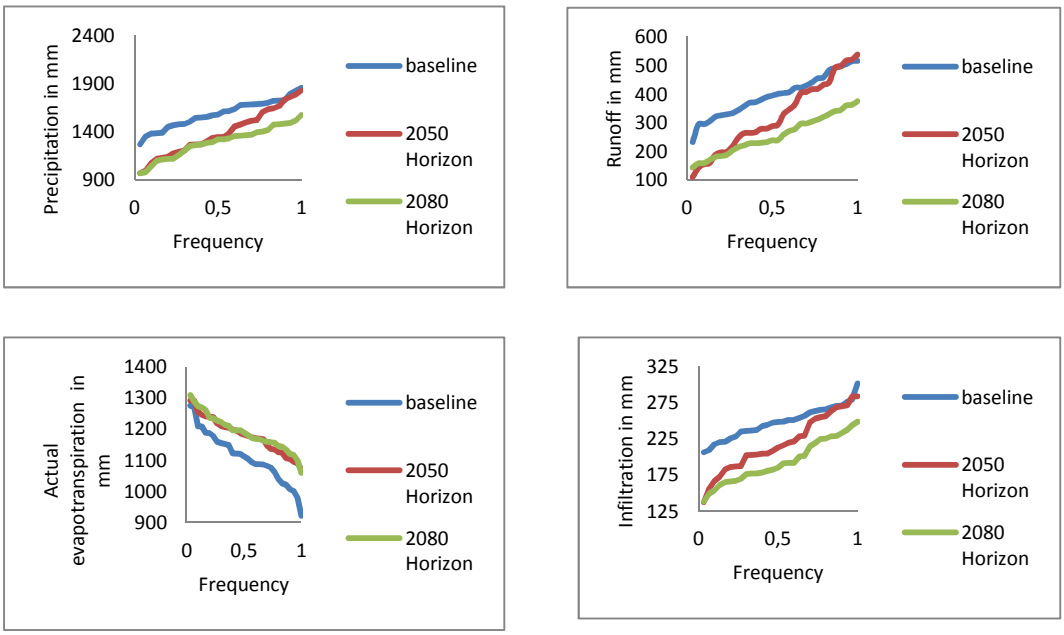

Fig. 18 Possible changes of water balance in the Buyo Lake watershed during the 2050s and 2080s

5 CONCLUSIONS

This study focused on the potential impacts of climate change on water resources showed that the watershed of Buyo Lake is vulnerable to climate change. Indeed, compared to the reference period 1950-1979, the scenario used provides variations in monthly temperatures between 0 and +1.34°C for the period 2035-2064 and +0.83 to +3.87°C for the period 2064-2093. These circumstances would lead the watershed to be warmer. A lower annual rainfall of 10.27% in 2050 (2035-2064) and 14.90% in 2080 (2064-2093) is estimated. Unlike precipitation, annual average actual evapotranspiration (ETR) could increase to 3.59% in the 2050s and to 3.44% in the 2080s. In terms of average annual runoff in this century, the expected deficits are more important than precipitation. Variations of -27.73% (339.81 mm / year to 245.58 mm / year) in 2050 and of -39.95% (339.81 mm / year to 204.04 mm / year) in the 2064-2093 period are provided. Water infiltration to groundwater would also suffer of reducing. Indeed, one could go from 249.90 to 164.45 mm water infiltrated in the 2050s, with a change of -34.19% over this period. In 2080s, a decrease of 45.81% is also planned. These decreases can cause a drying up of some hydraulic structures capturing groundwater during dry periods of the year. The study of potential impacts of climate change on water resources in the basin of Lake Buyo has highlighted the increasing climate variability directly influencing the water cycle. These changes pose a real threat to the livelihoods of the most disadvantaged populations. Thus, strategies for adaptation to climate change must take into account this reality and focus on improving the sustainable

exploitation of natural resources, in order to increase the resilience of ecosystems and reduce their vulnerability to risks and dangers. The results of this study allow getting an idea of the evolution of the parameters of the water balance of the whole watershed. These results provide a valid working hypothesis it would be necessary to refine progressively as performances of climate model will improve

REFERENCES

[1] P. Hubert, J. P. Carbonel, A. Chaouche, "Segmentation of hydrometeorological series. Application to a series of precipitation and flow of West Africa'', *Journal of Hydrology*, vol. 110, pp. 349-367, 1989. (In French)

[2] G. Mahé and C. Olivry, "Variations in rainfall and runoff in West Africa and Central from 1951 to 1989", *Sécheresse*, vol. 6, no. 1, pp. 109-17, 1995. (In French)

[3] J. P. Bricquet, F. Bamba, G. Mahe, M. Toure and J. C. Olivry, "Variability of water resources in Atlantic Africa", *IHP-V*, vol. 6, pp. 83-95, 1997. (In French)

[4] E. Servat, J. E. Paturel, H. Lubes, B. Kouame, J. M. Masson, M.Travaglio, B. Marieu, "Different aspects of the variability of rainfall in West Africa and Central Sahel", *Journal of Water Science*, vol. 12, no. 2, pp. 363-387, 1999. (In French)

[5] IPCC, "Climate Change and Water", *IPCC Technical Report IV*, 214 p, 2008.

[6] IUCN, Reduce the vulnerability of West Africa to climate impacts on water resources, wetlands and desertification, 2004. [Online] Available: www.iucn.org/bookstore (January, 12, 2013). (In French)

[7] K. Kouakou, "Impacts of climate variability and climate change on water resources in West Africa: the case of Comoé watershed (Ivory Coast)", PhD thesis, *University of Abobo-Adjamé*, 186 p, 2011. (In French)

[8] I. S. Sanda, "Climate scenarios on the West Africa: performance of IPCC models on West africa", *proceedings of the International Symposium*, Niamey, May, 2009. (In French)

[9] J. E. Paturel, E. Servat, B. Kouame, H. Lubes, J. M. Masson, J. Boyer, F. Travaglio, M. M. Marieu, "Rainfall variability in humid Africa along the Gulf of Guinea, integrated regional approach", *IHP-V*, vol. 16, pp. 1-31, 1997. (In French)

[10] A. A. Aka, H. Moons, M. Masson, E. Servat, J. E. Paturel, B. Kouamé, "Analysis of the temporal evolution of flows in Ivory Coast. Statistical approach and characterization of phenomena", *IHP-V*, vol. 16, pp. 49-63, 1997. (In French)

[11] T. Brou, E. Servat, J. E. Paturel, "Human activities and climate variability: the case of southern Ivorian forest", *IAHS*, vol. 252, pp. 365-373, 1998 (In French)

[12] I. Savané, K. Coulibaly, P. Gioan, "Climate variability and groundwater resources in the semi-mountainous region of Man", *Sécheresse*, vol. 12, No. 4, pp. 231-237, 2001 (In French)

[13] C. B. Péné, D. A. Assa, "Interannual variations in rainfall and water supply for sugarcane in Ivory Coast", *Sécheresse*, vol. 14, no. 1, pp. 43-52, 2003 (In French)

[14] B. Saley, "Hydrogeological spatial reference information system, pseudo-images discontinuities and thematic maps for water resources in the semi-mountainous region of Man (Western Ivory Coast)", PhD thesis, *University of Cocody*, 209 p, 2003. (In French)

[15] (MEEF, Forest, Water and Environment Ministry), "Initial National Communication of Ivory Coast, prepared under the UN Convention on Climate Change Framework", *Report*, 97 p, 2000. (In French)

[16] B. T. A. Goula, I. Savannah, B. Konan, V. Fadika, G. B. Kouadio, "Impact of climate variability on water resources N'Zo and N'Zi basins in Ivory Coast (tropical Africa)", *VertigO - electronic Environmental Science journal*, Vol. 7, no. 1, 12 p, 2006. (In French)

[17] B. Yao, "Evolution of rainfall and deforestation in south-west and central Ivory Coast", *Notes and works, ORSTOM*, No. 8, 1998. (In French)

[18] Uehara and Gillman, *The mineralogy, chemistry, and physics of tropical soils with variable charge clays*, Westview press tropical agricultural series, Westview press, Inc., Boulder, 1981.

[19] T. J. Koua, J. P. Jourda, K. J. Kouamé, K. A. Anoh, "Assessment of Sediments and Pollutants in Buyo Lake, Ivory Coast, Using SWAT (Soil and Water Assessment Tool) Model", *Journal of Chemistry and Chemical Engineering*, David Publishing Company, Vol. 7, no. 11, pp. 1054-1059, 2013.

[20] F. Nachtergaele, H. V. Velthuizen, L. Verest, "Harmonized world soil database version 1. 1", 20 p, 2009

[21] Anonymous, Surface hydrology, B2a - Hydrology of the metropolis, 2012. [Online] Available: http://www.developpementdurable.gouv.fr/IMG/pdf/Etude_modelisation_hydrologique_metropole.pdf (February, 2014). (In French)

[22] J. G. Arnold and N. Fohrer, "Current capabilities and research opportunities in applied watershed modeling", *Hydrolog. Processes*, Vol. 19, pp. 563-572, 2005.

[23] K. C. Abbaspour, "SWAT- Calibration and uncertainty programs", a user manual, *Eawag: Swiss Federal institute of aquatic science and technology*, 103 p, 2011.

[24] M. Thiébualt, "Hydrological modeling of a climate change scenario on the Bani watershed with SWAT", Master, *ENGEES (National School of Engineers in Water and Environment of Strasbourg)*, 55 p, 2010. (In French)
[25] L. K. Smedema and D.W. Rycroft, Land drainage planning and design of agricultural drainage systems", Cornell university press, Ithica, 1983.
[26] M. D. McKay, R. J. Beckman, W. J. Conover, "A comparison of three methods for selecting values of input variables in the analysis of output from a computer code", *Technometrics*, Vol. 21, pp. 239-245, 1979.
[27] W. H. Press, B. P. Flannery, S. A. Teukolsky, W. T. Vetterling, *Numerical Recipe, the Art of Scientific Computation*, 2nd ed. Cambridge University Press, Cambridge, Great Britain, 1992.
[28] C. Santhi, J.G. Arnold, J.R. Williams, W. A. Dugas, R. Srinivasan, L. M. Hauck, "Validation of the SWAT model on a large river basin with point and nonpoint sources", *Journal of American Water Resources Association*, vol. 37, no .5, pp. 1169-1188, 2001.
[29] M. W. Van Liew, J. G. Arnold, J. D. Garbrecht, "Hydrology simulation on agricultural watersheds: Choosing between two models", *Transactions ASAE*, vol. 46, no. 6, pp. 1539-1551, 2003.
[30] S. Eisner, F. Voss, E. Kynast, Statistical bias correction of global climate projections–consequences for large scale modeling of flood flows, 2012. *Advances in Geosciences*, [Online] Available: www.advgeosci.net/31/75/2012/ (October, 2013).
[31] ECOWAS-SWAC, "Climate and climate change in West Africa", *Atlas of regional integration in West Africa*, *CSAO/OCDE, ILSS, FAO*, 13 p. 2008. (In French)
[32] B. S. Ardoin, "Hydroclimatic variability and impacts on water resources in large river basins in the Sudano-Sahelian zone. PhD thesis, *University of Montpellier II*, 440 p, 2004. (In French)